Sulfur isotopes of host strata for Howards Pass (Yukon-Northwest Territories) Zn-Pb deposits implicate anaerobic oxidation of methane not basin stagnation

Craig A. Johnson[1], John F. Slack[2], Julie A. Dumoulin[3], Karen D. Kelley[1], and Hendrik Falck[4]

[1]*U.S. Geological Survey, P.O. Box 25046, Denver, Colorado 80225, USA*

[2]*U.S. Geological Survey (Emeritus), National Center, MS 954, Reston, Virginia 20192, USA*

[3]*U.S. Geological Survey, Alaska Science Center, Anchorage, Alaska 99508, USA*

[4]*Northwest Territories Geological Survey, P.O. Box 1320, Yellowknife, NT X1A 2L9, Canada*

METHODS

Mudstones were sampled from drill holes XYC–116 in the core of the XY Central zone and XYC–167 in the southeast margin of the zone (see Slack et al., 2017). Additional samples were obtained from drill hole cores in the XY Central (XYC–115), Don (D–197), and Don East (DNE–106) zones. Core pieces weighing a few tens of grams to a few hundred grams were powdered in a ceramic mortar and pestle for chemical, S isotope, and C isotope analysis. Five concretions were sampled by microdrilling of pyrite or calcite, and were analyzed only for S and C isotopes. Iron, Zn, Pb, Al, and organic carbon (C_{org}) concentrations were determined by Activation Laboratories, Ltd., Acton, Ontario. Metal concentrations were determined by inductively-coupled plasma mass spectrometry after fusing the powders with lithium metaborate/tetraborate flux and dissolving the resulting glasses in acid. Organic C was determined by induction-furnace infrared analyzer after acid removal of carbonate carbon. Pyrite S was extracted from aliquots of powder weighing 0.2 g by the chromium chloride method

(Canfield et al., 1986). The S yield, which was obtained by weighing the end product Ag_2S, was used to calculate the concentration of pyrite S. The Ag_2S was then analyzed by elemental analyzer-isotope ratio mass spectrometry (EA-IRMS) to obtain the sulfur isotope composition of total pyrite (Johnson et al., 2018). The EA-IRMS was calibrated by analyzing the IAEA-S-3 and NBS 123 standards, the accepted compositions for which were taken from Brand et al. (2014). Carbonate C isotopes were analyzed by phosphoric acid digestion using either septum-capped vials in an autosampler or stopcock-sealed reaction vessels (McCrea, 1950). Metallic Ag was suspended in the vessels to eliminate any H_2S from pyrite decomposition. The procedures were calibrated by analyzing the NBS 18 and NBS 19 calcite standards (accepted compositions from Brand et al., 2014) or in-house calcite standards that had been calibrated against NBS 18 and NBS 19. Isotopic results are expressed as δ-values where $\delta^{34}S$ (in per mil, ‰) = $((^{34}S/^{32}S_{sample}/^{34}S/^{32}S_{VCDT}) - 1) \times 1{,}000$, and $\delta^{13}C$ (in per mil, ‰) = $((^{13}C/^{12}C_{sample}/^{13}C/^{12}C_{VPDB}) - 1) \times 1{,}000$. Duplicate analyses generally agreed to within ± 0.2 ‰ for $\delta^{34}S$ and within ± 0.1 ‰ for $\delta^{13}C$.

REFERENCES CITED

Brand, W.A., Coplen, T.B., Vogl, J., Rosner, M., and Prohaska, T., 2014, Assessment of international reference materials for isotope-ratio analysis (IUPAC Technical Report): Pure and Applied Chemistry, v. 86, p. 425–467, https://doi:10.1515/pac-2013-1023.

Canfield, D.E., Raiswell, R., Westrich, J.T., Reaves, C.M., and Berner, R.A., 1986, The use of chromium reduction in the analysis of reduced inorganic sulfur in sediments and shales: Chemical Geology, v. 54, p. 149–155, doi:10.1016/0009-2541(86)90078-1.

Johnson, C.A., Stricker, C.A., Gulbransen, C.A., and Emmons, M.P., 2018, Determination of $\delta^{13}C$, $\delta^{15}N$, or $\delta^{34}S$ by isotope-ratio-monitoring mass spectrometry using an elemental analyzer: U.S. Geological Survey Techniques and Methods, 5-D4, https://doi:10.3133/tm5D4.

Lyons, T.W., and Severmann, S., 2006, A critical look at iron paleoredox proxies: new insights from modern euxinic marine basins: Geochimica et Cosmochimica Acta, v. 70, p. 5698–5722, https://doi:10.1016/jgca.2006.08.021.

McCrea, J.M., 1950, On the isotope chemistry of carbonates and a paleotemperature scale: Journal of Chemical Physics, v. 18, p. 849–857.

Scott, C., and Lyons, T.W., 2012, Contrasting molybdenum cycling and isotopic properties in euxinic versus non-euxinic sediments and sedimentary rocks: refining the paleoproxies: Chemical Geology, v. 324–325, p. 19–27, https://doi:10.1016/j.chemgeo.2012.05.012.

Slack, J.F., Falck, H., Kelley, K.D., and Xue, G.G., 2017, Geochemistry of host rocks in the Howards Pass district, Yukon-Northwest Territories, Canada: implications for sedimentary environments of Zn-Pb and phosphate mineralization: Mineralium Deposita, v. 52, p. 565–593, https://doi:10.1007/s00126-016-0680-x.

FIGURE CAPTION

Figure DR1. Plots showing relationships among redox proxies for the Duo Lake Formation: A, concentration of Mo versus degree of pyritization of total Fe (DOP_T = pyrite-Fe/total-Fe); B, concentration of Mo versus Fe/Al; and C; Fe/Al versus DOP_T. Mo > 25 ppm is normally considered diagnostic of at least intermittent euxinia; higher Fe/Al and DOP_T are normally considered diagnostic of more reducing conditions culminating in euxinia (Scott and Lyons, 2012; Lyons and Severmann; 2006). Data presented in Table DR1.

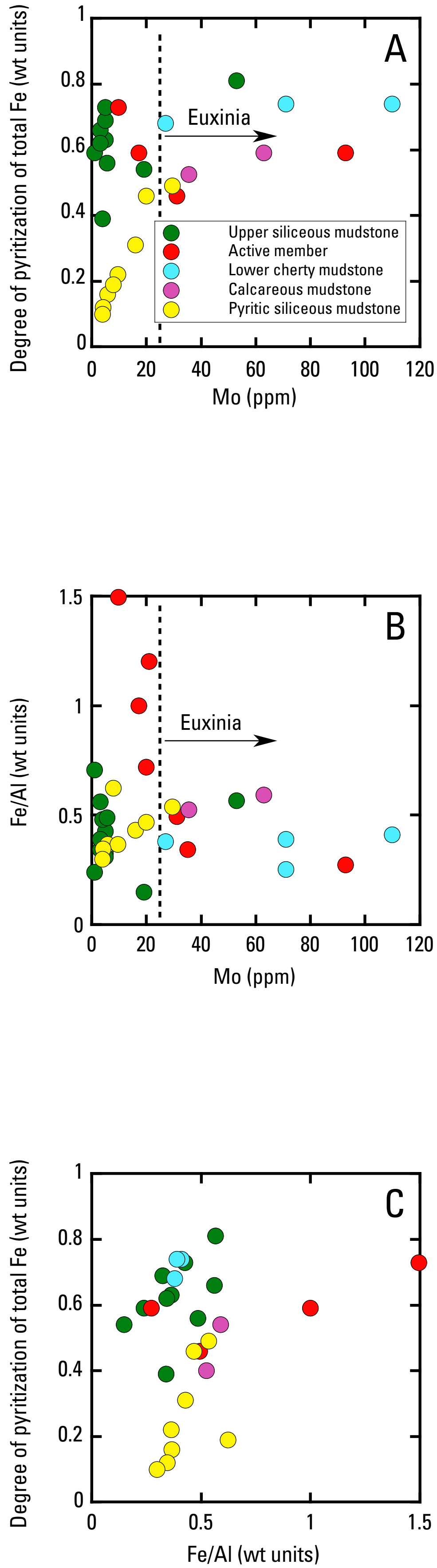
A
B
C
Euxinia
Upper siliceous mudstone
Active member
Lower cherty mudstone
Calcareous mudstone
Pyritic siliceous mudstone
Degree of pyritization of total Fe (wt units)
Fe/Al (wt units)
Mo (ppm)

Table DR1. Isotopic and chemical data for samples of Duo Lake Formation.

Sample*	Member †	Lithology	Pyrite S (%)	Organic C (%)	δ34S-pyrite (‰)	δ13C-carbonate (‰)	Fe (%)	Al (%)	Mo (ppm)	Zn (ppm)	Pb (ppm)	DOP-total§
XYC-116-202.3	usm	mudstone	1.94	5.86	11.8		2.67	7.37	5	19	36	0.63
XYC-116-204.2	usm	phosphatic mudstone	0.56	6.44	30.6		1.24	3.66	4	9	21	0.39
XYC-116-206.9	usm	phosphatic mudstone	0.80	6.74	29.5		1.18	4.96	<2	10	10	0.59
XYC-116-212.5	usm	phosphatic mudstone	1.40	7.32	33.1	-6.5	1.84	3.28	3	12	44	0.66
XYC-116-220.5	usm	phosphatic mudstone	1.16	8.23	29.6		1.46	4.49	5	64	89	0.69
XYC-116-225.0	usm	phosphatic mudstone	1.34	10.05	38.4		1.61	3.79	5	780	59	0.72
XYC-116-225.5	usm	phosphatic mudstone	1.84	7.55	32.3		1.24	2.59	4	18100	52	
XYC-116-234.5	usm	mudstone	0.72	6.74	22.2		1.00	2.93	3	82	18	0.63
XYC-116-266.2	usm	mudstone	0.78	6.97	21.1		0.67	1.72	3	6720	72	
XYC-116-286.3	usm	siliceous mudstone	0.21	1.12	27.7		0.26	0.37	<2	2170	76	
XYC-116-288.0	usm	siliceous mudstone	0.29	7.39	22.2		0.33	1.07	5	1270	96	
XYC-116-290.0	usm	mudstone	1.36	5.74	18.3	-4.2	1.46	2.58	53	20	135	0.81
XYC-116-300.5	usm	limestone			25.2	-4.4						
XYC-116-304.8	usm	siliceous mudstone	0.15	6.01	13.9		0.24	1.63	19	136	67	0.54
XYC-116-316.2**	usm	siliceous mudstone	0.34	6.14	22.1		0.54	1.11	5.50	919	68.1	0.55
XYC-116-323.8**	am	mudstone	0.53	7.88	-0.6	-4.8	0.78	0.78	17.2	296	186	0.59
XYC-116-325.4	am	siliceous mudstone	1.18	6.68	13.1		1.10	1.63	21	21300	3600	
XYC-116-326.2**	am	highly carbonaceous mudstone	0.50	16.48	-3.9		0.73	2.69	92.8	296	250	0.59
XYC-116-326.8	am	mudstone	0.61	7.98	7.0		0.40	1.17	35	8240	1690	
XYC-116-334.2**	am	siliceous mudstone	1.32	2.37	15.3	-3.5	1.57	1.05	9.81	668	330	0.73
XYC-116-350.1	am	mudstone	0.78	6.16	12.1	-3.7	0.87	1.21	20	75	2320	0.78
XYC-116-357.6**	am	mudstone	0.36	6.73	-5.2		0.66	1.34	31.2	25.5	174	0.47
XYC-116-364.7	lcm	limestone			16.4	-3.9						
XYC-116-365.0	lcm	limestone			17.2	-6.3						
XYC-116-365.7	lcm	limestone			20.0	-11.7						
XYC-116-370.3	lcm	siliceous mudstone	0.27	8.22	14.6		0.28	1.11	71	2670	160	
XYC-116-376.5	lcm	highly carbonaceous mudstone	1.73	13.20	5.6	-3.4	2.02	4.92	110	115	253	0.75
XYC-116-380.3	lcm	mudstone	1.30	8.31	4.3		1.66	4.38	27	12	46	0.68
XYC-116-393.2	lcm	mudstone	1.21	7.81	4.3		1.42	3.64	71	285	65	0.74
XYC-167-281.0**	ccm	mudstone	1.97	3.40	-5.7	-4.1	3.20	5.43	63.0	20.2	27.3	0.54
XYC-167-285.5**	ccm	mudstone	1.23	2.54	-6.3	-4.2	2.68	5.11	35.6	351	19.3	0.40
XYC-167-300.0**	psm	mudstone	1.78	1.45	-5.6	-4.1	3.19	5.95	29.6	20.3	35.7	0.49
XYC-167-310.5**	psm	dolomitic mudstone	1.02	1.32	-8.4	-3.9	2.87	6.69	16.0	13.8	23.4	0.31
XYC-167-318.1**	psm	mudstone	1.57	1.34	-5.5	-4.1	2.97	6.36	19.9	11.8	34.4	0.46
XYC-167-328.9**	psm	dolomitic mudstone	0.32	0.64	-5.1	-3.5	1.76	4.81	5.82	15.1	7.47	0.16
XYC-167-337.2**	psm	dolomitic mudstone	0.49	0.75	-8.6	-3.7	1.92	5.27	9.60	89.4	6.9	0.22
XYC-167-345.7**	psm	dolomitic mudstone	0.24	0.54	-7.8	-3.5	1.78	5.17	4.22	39.8	9.56	0.12
XYC-167-358.1**	psm	dolomitic mudstone	0.54	0.59	-16.0	-3.6	2.47	3.96	7.85	24.4	14.6	0.19
XYC-167-363.6**	psm	mudstone	0.17	0.98	-15.4	-3.7	1.56	5.22	3.82	287	7.47	0.09
XYC-115-61.0	usm	limestone				-2.5						
XYC-115-72.9	usm	limestone			-1.0	-3.8						
D197-410 † †	usm	concretion			34.5	-12.2						
D197-432.2A † †	usm	concretion				-9.8						
D197-432.2B † †	usm	concretion			27.9	-10.1						
D197-612.85 † †	ccm	concretion			13.0							
DNE106-280.9 † †	usm	concretion			26.5	-8.7						

* Sample numbers consist of zone (XYC = XY Central, D = Don, DNE = Don East), drill hole number, and depth, in meters.

† usm = upper siliceous mudstone, am = active member, lcm = lower cherty mudstone, ccm = calcareous mudstone, psm = pyritic siliceous mudstone.

§ DOP-total = pyrite Fe/total Fe, where pyrite Fe = 0.861 * pyrite S. No value given where Zn or Pb exceed 1,000 ppm due to possibile bias from sphalerite or galena contributions to pyrite S.

**Analyses of same powders analyzed by Slack et al. (2017). Values for Fe, Mo, Zn, Pb, and organic C are from those authors. For other samples, new pieces of core were powdered for isotopic and chemical analysis.

† † Powders obtained using a dental drill.